O-GlcNAcylation destabilizes the active tetrameric PKM2 to promote the Warburg effect

Yang Wang[a,1], Jia Liu[a,1], Xin Jin[a,1], Dapeng Zhang[b,c], Dongxue Li[a], Fengqi Hao[a], Yunpeng Feng[a], Shan Gu[a], Fanlin Meng[a], Miaomiao Tian[a], Yi Zheng[a], Ling Xin[a], Xinbo Zhang[a], Xue Han[a], L. Aravind[d], and Min Wei[a,2]

[a]Key Laboratory of Molecular Epigenetics of the Ministry of Education, Northeast Normal University, Changchun, Jilin, 130024, People's Republic of China; [b]Department of Biology, Saint Louis University, St. Louis, MO 63103; [c]Program of Bioinformatics and Computational Biology, Saint Louis University, St. Louis, MO 63103; and [d]National Center for Biotechnology Information, National Library of Medicine, National Institutes of Health, Bethesda, MD 20894

Edited by Gregg L. Semenza, Johns Hopkins University School of Medicine, Baltimore, MD, and approved November 13, 2017 (received for review March 14, 2017)

The Warburg effect, characterized by increased glucose uptake and lactate production, is a well-known universal across cancer cells and other proliferating cells. PKM2, a splice isoform of the pyruvate kinase (PK) specifically expressed in these cells, serves as a major regulator of this metabolic reprogramming with an adjustable activity subjected to numerous allosteric effectors and posttranslational modifications. Here, we have identified a posttranslational modification on PKM2, *O*-GlcNAcylation, which specifically targets Thr^{405} and Ser^{406}, residues of the region encoded by the alternatively spliced exon 10 in cancer cells. We show that PKM2 *O*-GlcNAcylation is up-regulated in various types of human tumor cells and patient tumor tissues. The modification destabilized the active tetrameric PKM2, reduced PK activity, and led to nuclear translocation of PKM2. We also observed that the modification was associated with an increased glucose consumption and lactate production and enhanced level of lipid and DNA synthesis, indicating that *O*-GlcNAcylation promotes the Warburg effect. In vivo experiments showed that blocking PKM2 *O*-GlcNAcylation attenuated tumor growth. Thus, we demonstrate that *O*-GlcNAcylation is a regulatory mechanism for PKM2 in cancer cells and serves as a bridge between PKM2 and metabolic reprogramming typical of the Warburg effect.

PKM2 | *O*-GlcNAcylation | Warburg effect | cancer metabolism

Compared with normal cells, cancer cells have distinct metabolic features characterized by changes in nutrient consumption and metabolite concentrations (1). One prominent feature is aerobic glycolysis, which leads to increased glucose consumption and lactate production in cancer cells, a phenomenon referred to as the Warburg effect (2–5). It is believed that the Warburg effect not only allows cancer cells to meet high biosynthetic demand in both ATP and biomass production, but also provides a resistance to acid-induced cell toxicity, thus promoting unconstrained proliferation and invasion (6).

Recent studies have shown pyruvate kinase M2 (PKM2) to be a major regulator for metabolic reprogramming in cancer which contributes to the Warburg effect (7–9). Pyruvate kinases (PKs) are the final rate-limiting enzymes in glycolysis. In humans, two PK genes generate four isoforms via alternative splicing, PKL, PKR, PKM1, and PKM2, which display distinct tissue-specific expression patterns (10, 11). The PKL and PKR isoforms are expressed in liver and red blood cells, respectively. PKM1, containing exon 9 of the PKM gene, is expressed in most adult tissues, whereas PKM2, containing exon 10, is expressed during embryonic development and in other highly proliferative cells, including cancer cells (2, 4, 11). The expression switch from PKM1 to PKM2 is frequently observed in many cancer cells and is critical for cancer cell proliferation (7).

The mechanism for this switch from PKM1 to PKM2, which induces metabolic reprogramming and the Warburg effect in cancer cells, remains largely unclear. It appears that, although the difference between PKM1 and PKM2 is only 22 amino acids, PKM2 displays a very unique regulatory property: whereas PKM1 forms a stable, constitutively active tetramer, PKM2's tetrameric status and activity are closely controlled by numerous allosteric effectors and posttranslational modifications. On the one hand, PKM2 is allosterically activated by fructose 1,6-bisphosphate (FBP) (12), an upstream intermediate in glycolysis, and serine, which is synthesized from a glycolytic intermediate 3-phosphoglycerate (13). On the other hand, PKM2 activity is regulated by several posttranslational modifications, such as phosphorylation, acetylation, and SUMOylation (14–19). These modifications, such as acetylation on Lys^{433} or phosphorylation on Tyr^{105}, impair PKM2 activity by blocking the association of FBP (16, 17). Furthermore, several modifications are frequently associated with the translocation of PKM2 from cytoplasm to nucleus, where a nonmetabolic function of PKM2 is critical in the establishment of the Warburg effect (16, 20). Thus, it appears that the permissive property of PKM2 function regulated by allosteric effectors and posttranslational modifications and its nuclear function allow PKM2 to serve as a key regulatory node in metabolic reprogramming in cancer cells (21).

O-GlcNAcylation of enzymes has been recently implicated as an important regulatory mechanism for metabolic pathways (22). Two enzymes, phosphofructokinase 1 (PFK1) and glucose-6-phosphate dehydrogenase (G6PD), have been shown to undergo *O*-GlcNAcylation to regulate cell metabolism and proliferation (23, 24). In the present study, we investigated whether the key metabolic regulator in cancer cells, PKM2, is also modified by *O*-GlcNAcylation and examined its potential role in the Warburg effect. We discovered that, across diverse tumor cell types and patient tissues, PKM2 was *O*-GlcNAcylated at two residues, Thr^{405}

Significance

Cancer cells are characterized by a high rate of glycolysis even under normal oxygen availability to meet the demand of biomass production during rapid proliferation. An isoform of pyruvate kinase (PK), PKM2, preferentially expressed in cancers, was recently shown to be critical for this metabolic reprogramming with adjustable activity and dynamic cellular relocalization. However, specific molecular mechanisms mediating PKM2's role in cancer-specific metabolism remain largely elusive. We demonstrate that *O*-GlcNAcylation of PKM2 on threonine/serine encoded by an alternatively spliced exon disrupts the intersubunit interactions in the active PKM2 tetramer. This causes the tetramer disassembly, reduced PK activity, and its nuclear translocation to facilitate cell proliferation. Thus, our findings furnish a key piece in the puzzle of aerobic glycolysis in cancer.

Author contributions: Y.W., J.L., X.J., Y.F., and M.W. designed research; Y.W., J.L., X.J., D.L., F.H., S.G., F.M., M.T., Y.Z., L.X., X.Z., and X.H. performed research; Y.W., J.L., X.J., D.Z., and D.L. contributed new reagents/analytic tools; Y.W., J.L., X.J., D.Z., D.L., F.H., Y.F., and M.W. analyzed data; and Y.W., D.Z., Y.F., L.A., and M.W. wrote the paper.

The authors declare no conflict of interest.

This article is a PNAS Direct Submission.

[1]Y.W., J.L., and X.J. contributed equally to this work.

[2]To whom correspondence should be addressed. Email: weim750@nenu.edu.cn.

This article contains supporting information online at www.pnas.org/lookup/suppl/doi:10.1073/pnas.1704145115/-/DCSupplemental.

and Ser^{406}, of the region encoded by spliced exon 10. This modification detetramerized the active PKM2 and led to a dramatically reduced activity and increased nuclear translocation. We also observed that PKM2 *O*-GlcNAcylation promoted the Warburg effect with an increased glucose consumption and lactate production. Thus, we demonstrated that *O*-GlcNAcylation is a regulatory mode for PKM2 in cancer cells and serves as a bridge translating genomic switch from PKM1 to PKM2 toward metabolic reprogramming.

Results

PKM2 Is Highly *O*-GlcNAcylated in Tumor Cells and Patient Tumor Tissues. We first set out to investigate PKM2 *O*-GlcNAcylation in different proliferating cell types, including activated T, Jurkat, MCF-10A, MCF-7, MDA-MB-231, HEK-293T, HeLa, A375, T98-G, U251, and U937. PKM2 expression and global *O*-GlcNAcylation were pronounced in proliferating cells, but not in quiescent naive T cells (Fig. 1*A*). Furthermore, through two different methods (Click-iT *O*-GlcNAc Enzymatic Labeling and traditional immunoprecipitation), PKM2 *O*-GlcNAcylation was detected in all tested cells, and it was strongly up-regulated in malignant cell lines derived from leukemia and solid tumors compared with untransformed cells, including naive T, activated T, MCF-10A, and HEK-293T (Fig. 1*B* and Fig. S1*A*). Notably, no difference was found between activated T cells and their quiescent counterparts (Fig. 1*B* and Fig. S1*A*). These data indicate that the up-regulation of PKM2 *O*-GlcNAcylation might have a specific role in cancer cell proliferation.

We further examined the level of *O*-GlcNAcylation of PKM2 in both breast tumor tissues and tumor-adjacent normal tissues from the same patient. By studying a wide range of patient samples, we found that PKM2 *O*-GlcNAcylation was significantly elevated in breast tumor tissues compared with adjacent normal tissues (Fig. 1 *C* and *D* and Fig. S1*B*). The enhanced signal of PKM2 *O*-GlcNAcylation was also consistent with the up-regulated expression of PKM2 in tumor tissues compared with adjacent tissues (Fig. S1*C*). These results strongly indicate that, not only the high expression of PKM2 in tumor cells, but also *O*-GlcNAcylation of PKM2, is a characteristic feature for tumor cells.

We examined the stoichiometry of PKM2 *O*-GlcNAcylation using two chemoenzymatic labeling methods (a Click-iT biotinylation and an Alkyne-5K-PEG resolvable mass tag) (25, 26); both revealed that the basal *O*-GlcNAcylation level of PKM2 in MCF-7 cells was ∼7–10% (Fig. S2 *A* and *B*).

PKM2 Is *O*-GlcNAcylated at Thr^{405} and Ser^{406}. We next sought to identify the *O*-GlcNAcylation site(s) on PKM2. In *Escherichia coli* cotransfected with GST-tagged PKM2 and *O*-GlcNAc transferase (OGT), Thr^{405} and Ser^{406} were detected as *O*-GlcNAcylation sites by mass spectrometry (Fig. 2*A*). Importantly, these two residues were located at the region encoded by exon 10, which is specifically introduced in the PKM2 transcript via alternative splicing in cancer cells (Fig. 2*A*). When Thr^{405} or Ser^{406} was mutated into alanine (PKM2^{T405A} or PKM2^{S406A}), the *O*-GlcNAcylation level of PKM2 in MCF-7 cells was decreased (Fig. 2*B*). The reduction of PKM2 *O*-GlcNAcylation was more pronounced when Thr^{405} and Ser^{406} were both mutated (PKM2$^{T405A/S406A}$) (Fig. 2*B*). We next investigated the issue of *O*-GlcNAcylation of PKM2 not being completely abolished in these mutants by further exploring other potential *O*-GlcNAcylation residues. By studying the available PKM2 crystal structure (27), we selected all Ser and Thr residues located at the surface of the protein (total of 12 additional residues), which are theoretically accessible to OGT. However, mutating them to alanine did not substantially decrease the level of PKM2 *O*-GlcNAcylation as Thr^{405} or Ser^{406} did (Fig. S2*C*). Therefore, both mass spectrometry and extensive mutation studies suggested that Thr^{405} and Ser^{406} are the primary *O*-GlcNAcylation sites on PKM2.

We next overexpressed wild-type PKM2 (PKM2^{WT}) or PKM2$^{T405A/S406A}$ in a series of tumor cells, including MDA-MB-231, A375, U251, U2OS, T98-G, and HeLa. Compared with PKM2^{WT}, PKM2$^{T405A/S406A}$ displayed greatly reduced *O*-GlcNAcylation (Fig. 2*C*). Next, we compared PKM2^{WT} with PKM2$^{T405A/S406A}$ modification

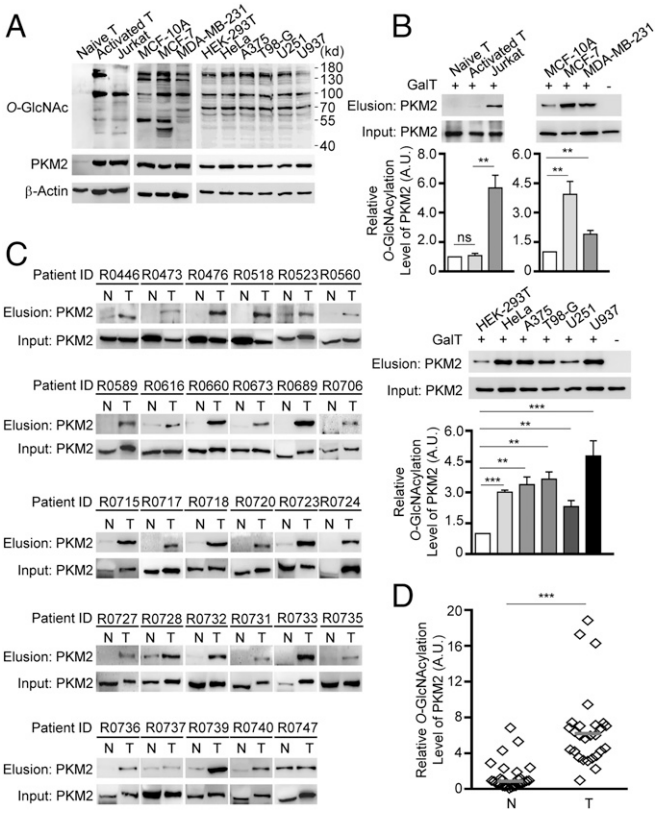

Fig. 1. PKM2 is highly *O*-GlcNAcylated in tumor cells and patient tumor tissues. (*A*) Detection of *O*-GlcNAc modification and PKM2 in human cell lines. The whole-cell lysates from indicated cells were analyzed by Western blotting (WB). All results shown in the study are representative of at least three independent experiments. (*B*) Detection of PKM2 *O*-GlcNAcylation in human cell lines by the Click-iT *O*-GlcNAc enzymatic labeling system. *O*-GlcNAcylated proteins were biotinylated, precipitated, and analyzed for PKM2 by WB. Relative PKM2 *O*-GlcNAcylation level (Elusion) was normalized to the total PKM2 protein level (Input) in each cell type. Error bars, SEM; $n = 3$ biological replicas. One-way analysis of variance (ANOVA) and Bonferroni comparison posttest: $^{**}P < 0.01$; $^{***}P < 0.001$; ns, nonsignificant. (*C*) Analysis of PKM2 *O*-GlcNAcylation in patient breast tumor tissues (T) and the matching adjacent normal tissues (N) by the Click-iT system. (*D*) The quantification of PKM2 *O*-GlcNAcylation level for *C*. Relative PKM2 *O*-GlcNAcylation level (Elusion) was normalized to total PKM2 (Input). Median is shown; $n = 29$. Student's *t* test: $^{***}P < 0.001$. A.U., arbitrary units; GalT, β-1,4-galactosyltransferase.

upon OGT overexpression or *O*-(2-acetamido-2-deoxy-D-glucopyranosylidene)amino-*N*-phenylcarbamate (PUGNAc) treatment, which up-regulates *O*-GlcNAcylation by inhibiting *O*-GlcNAcase (24, 28) (Fig. 2*D*). In both cases, a clear elevation of *O*-GlcNAcylation was detected in PKM2^{WT} (Fig. 2 *E* and *F*) or endogenous PKM2 (Fig. S3*A*), while poorly *O*-GlcNAcylated PKM2$^{T405A/S406A}$ only exhibited a limited change of *O*-GlcNAcylation under the same condition (Fig. 2 *E* and *F*). Stoichiometric analysis showed that, with PUGNAc, the *O*-GlcNAcylation level of PKM2 in MCF-7 cells was elevated to ∼13% (Fig. S2*B*). We also examined the *O*-GlcNAc modification of PKM2 in variable conditions. In response to a high supply of glucose or glutamine, *O*-GlcNAcylation was up-regulated in PKM2^{WT}, while no evident changes were observed in PKM2$^{T405A/S406A}$ (Fig. S4). Together, these results suggest that Thr^{405} and Ser^{406} are the dominant *O*-GlcNAcylation sites on PKM2 across diverse tumor cell types and that they are sensitive to fluctuations in nutritional supply.

O-GlcNAcylation Destabilizes PKM2 Tetramers and Reduces PK Activity. We then studied the impact of *O*-GlcNAcylation at Thr^{405} and Ser^{406} on PKM2 structure and function. Based on the crystal structure of PKM2 (27), we observed that Thr^{405} and Ser^{406}

CELL BIOLOGY

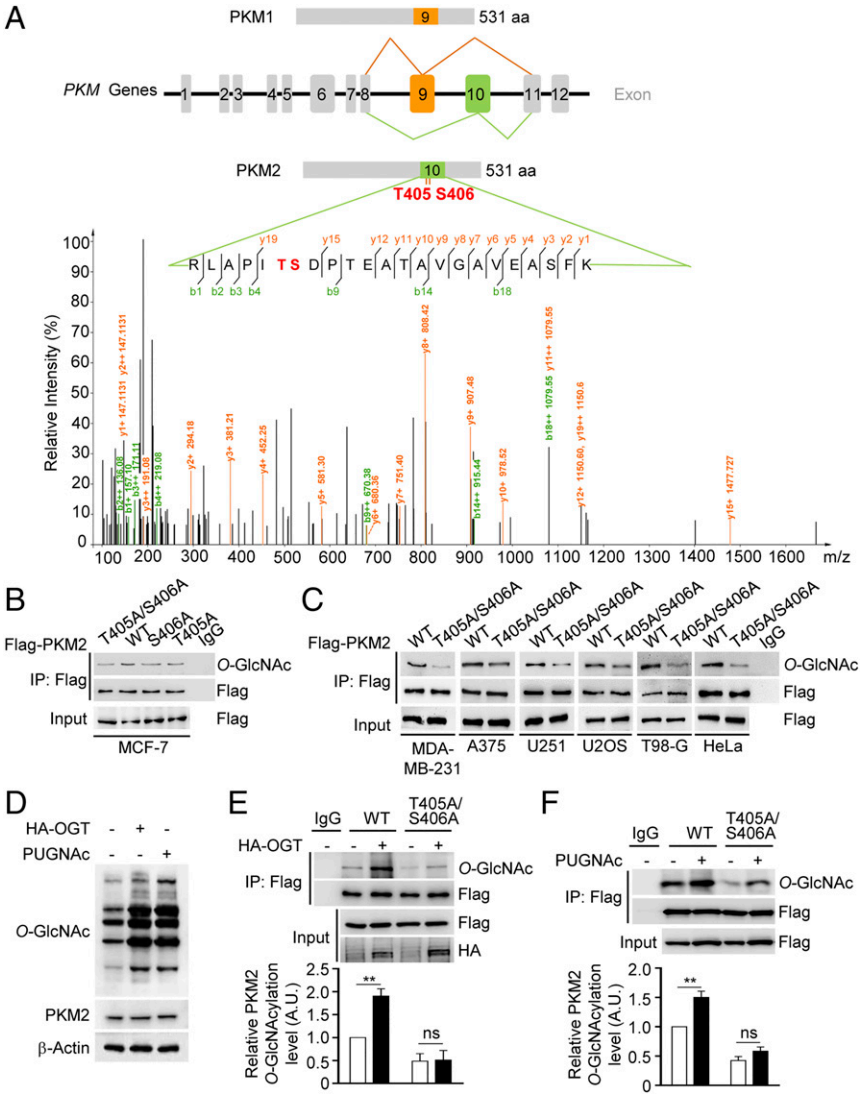

Fig. 2. PKM2 is *O*-GlcNAcylated at Thr^{405} and Ser^{406}. (*A*) Detection of the *O*-GlcNAcylation site(s) on PKM2. (*A*, *Upper*) A schematic depicting alternative splicing for *PKM* genes. The PKM1 and PKM2 isoforms are alternatively spliced forms of the *PKM* gene. They differ by the presence of either exon 9 (orange) in PKM1 or exon 10 (green) in PKM2. Thr^{405} and Ser^{406} of PKM2 are derived from exon 10. (*A*, *Lower*) GST-tagged human PKM2 and OGT were cotransfected in *E. coli*. The *O*-GlcNAc-modified peptides were enriched for LC-MS/MS analysis. The data were processed by using the MASCOT engine, which identified the *O*-GlcNAc peptide (RLAPITSDPTEATAVGAVEASFK). The y and b fragmentations were used to map the *O*-GlcNAcylation sites to the Ser and Thr indicated in red. (*B* and *C*) Confirmation of PKM2 *O*-GlcNAcylation at Thr^{405} and Ser^{406}. Flag-tagged PKM2^{WT}, PKM2^{T405A}, PKM2^{S406A}, or PKM2$^{T405A/S406A}$ was transfected into the indicated cell lines and immunoprecipitated for WB. (*D*) *O*-GlcNAcylation is up-regulated by OGT and PUGNAc. MCF-7 cells were transfected with HA-OGT or treated with PUGNAc. PKM2 and global *O*-GlcNAcylation were detected by WB. (*E* and *F*) OGT and PUGNAc up-regulate PKM2 *O*-GlcNAcylation through Thr^{405} and Ser^{406}. MCF-7 cells stably depleted for endogenous PKM2 by targeting shRNA and rescued by Flag-tagged PKM2^{WT} or PKM2$^{T405A/S406A}$ overexpression were transfected with HA-tagged OGT or treated with PUGNAc. Flag-PKM2–associated proteins were immunoprecipitated and analyzed by WB. Relative PKM2 *O*-GlcNAcylation level was normalized to the total PKM2 protein level for each group. A.U., arbitrary units. Error bars, SEM; $n = 3$ independent assays. Student's *t* test: $^{**}P < 0.01$; ns, nonsignificant.

were located N-terminal to an α-helix which formed a prominent part of the "C-C" interface during PKM2 tetramerization (29) (Fig. 3*A*). Thus, *O*-GlcNAcylation of Thr^{405} and Ser^{406} is likely to disrupt this tetramerization interface and thereby favors the dimeric or monomeric states of PKM2. Indeed, by modeling the PKM2 structure with *O*-GlcNAcylation at Thr^{405} and Ser^{406}, we found that one of the modified *O*-GlcNAc units, namely, that on Thr^{405}, can act as a direct barrier blocking a major stabilizing hydrogen bond of the C-C dimerization interface (Fig. 3*A*), which is formed between a lysine (Lys^{422}) from one monomer and a tyrosine (Tyr^{444}) from the counterpart monomer (also known as the peg-in-hole mechanism) (29). The second unit Ser^{406}, on the other hand, is likely to destabilize the oligomer further by interfering with other hydrophobic interactions (Movie S1). Thus, this strongly predicts that *O*-GlcNAc modification of PKM2 may induce disassociation of the tetramer by blocking the key interaction along the C-C interface.

We tested this prediction by investigating the effects of *O*-GlcNAcylation induced by PUGNAc or OGT overexpression on the tetrameric state of PKM2. Whereas the treatment dramatically reduced the tetramer level of both PKM2^{WT} (Fig. 3*B* and Fig. S5*A*) and endogenous PKM2 (Fig. S3*B*), the PKM2$^{T405A/S406A}$ tetramers were unaffected in the presence of PUGNAc (Fig. 3*B*) or OGT (Fig. S5*A*). Moreover, the level of PKM2$^{T405A/S406A}$ tetramers was close to that of PKM2^{WT} tetramers in the absence of PUGNAc (Fig. 3*B*). This confirmed that *O*-GlcNAcylation of Thr^{405} and Ser^{406} was critical for the disassociation of the PKM2 tetramer induced by PUGNAc or OGT overexpression. To further test the hypothesis that disruption of the Lys^{422}–Tyr^{444} interaction was central to the destabilizing of PKM2 tetramers (29), we constructed the single mutant PKM2^{K422A}. As predicted, disruption of the Lys^{422}–Tyr^{444} interaction by mutating Lys^{422} resulted in destabilization of the PKM2 tetramer, like what we observed with the *O*-GlcNAcylation of Thr^{405} and Ser^{406} (Fig. 3*C*). Thus, these results further support our hypothesis that *O*-GlcNAcylation at Thr^{405} and Ser^{406} destabilizes PKM2 tetramers and leads to a shift of the oligomeric equilibrium toward dimers and monomers.

It is known that tetramer conformation is required for the active PK activity of PKM2 (14, 16). We found that both PUGNAc and OGT overexpression resulted in a lowered PKM2 activity in PKM2^{WT} as opposed to *O*-GlcNAcylation–deficient PKM2$^{T405A/S406A}$ mutants (Fig. 3*D* and Figs. S3*C* and S5*B*). It should be noted that the mutant did not show an altered PKM2 activity with respect to the wild type, indicating that the mutations alone do not cause a loss of enzymatic activity (Fig. 3*D* and Figs. S5*B* and S6). Together, these data indicate that *O*-GlcNAc modification at Thr^{405} and Ser^{406} destabilizes PKM2 tetramers and reduces PK activity.

***O*-GlcNAcylation Is an Upstream Signal to Induce Nuclear Localization of PKM2.** In addition to the metabolic function in cytoplasm, recent studies have shown that PKM2 can migrate into the nucleus to play a

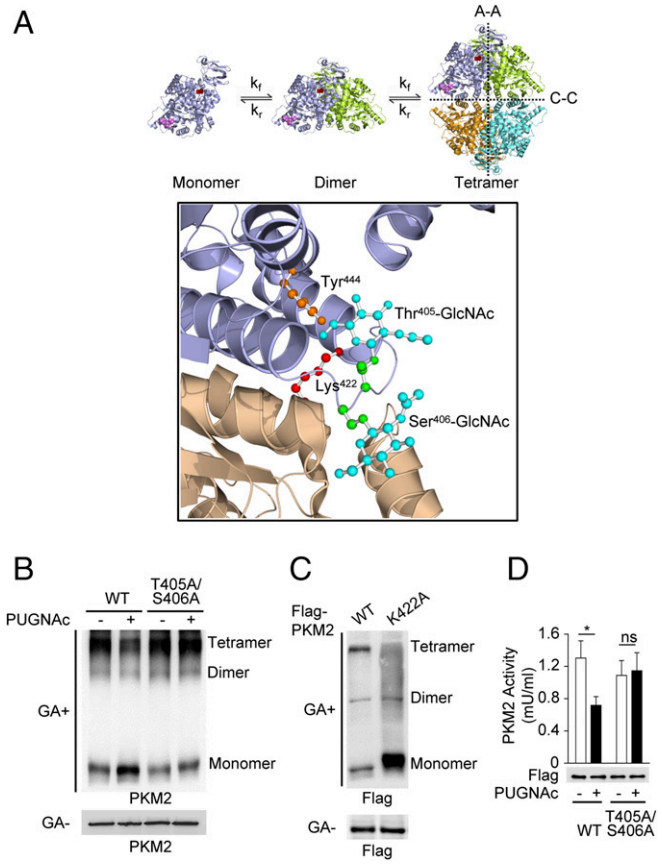

Fig. 3. *O*-GlcNAcylation destabilizes PKM2 tetramers. (*A*) Modeling of PKM2 structure with *O*-GlcNAcylation. (*A*, *Upper*) Dynamic equilibrium among monomers, dimers, and tetramers of PKM2. (*A*, *Lower*) Structural modeling shows that *O*-GlcNAc (blue) at Thr^{405} and Ser^{406} (green) disrupts the key stabilizing hydrogen bond between Lys^{422} (red) and Tyr^{444} (orange). (*B* and *C*) Change of PKM2 oligomer states upon *O*-GlcNAcylation. Transfection of Flag-tagged $PKM2^{WT}$, $PKM2^{T405A/S406A}$, or $PKM2^{K422A}$ along with or without concomitant PUGNAc treatment was conducted in PKM2-depleted MCF-7 cells. The whole-cell lysates were analyzed by WB. GA, glutaraldehyde. (*D*) *O*-GlcNAcylation regulates PKM2 activity. Enzymatic activity of $PKM2^{WT}$ and $PKM2^{T405A/S406A}$ was assayed. Error bars, SEM; $n = 3$ independent assays. Student's *t* test: $^*P < 0.05$; ns, nonsignificant.

nonmetabolic role in cancer cells (15, 16, 20, 30, 31). The migration is facilitated by the binding of importin α5, a nuclear translocation factor, to the nuclear localization signal (NLS) sequence of PKM2 (9, 15). We examined the impact of *O*-GlcNAcylation on the distribution of PKM2 in cells. Compared with cytoplasmic PKM2, nuclear PKM2 remained in a small amount (Fig. S7); however, it increased dramatically upon boosting of *O*-GlcNAcylation of PKM2 by PUGNAc (Fig. 4*A* and Figs. S3*D* and S7) or OGT overexpression (Fig. S5*C*). By contrast, the level of $PKM2^{T405A/S406A}$ was lower in the nucleus regardless of PUGNAc treatment (Fig. 4*A* and Fig. S7) or OGT overexpression (Fig. S5*C*). Consistent with this, immunofluorescence demonstrated that both $PKM2^{WT}$ (Fig. 4*B*) and endogenous PKM2 (Fig. S3*E*), but not $PKM2^{T405A/S406A}$ (Fig. 4*B*), accumulated in the nucleus in response to PUGNAc treatment. These suggest that the *O*-GlcNAcylation at Thr^{405} and Ser^{406} is important for the nuclear translocation of PKM2.

We next examined whether *O*-GlcNAcylation–induced PKM2 nuclear translocation involves the interaction of PKM2-NLS with importin α5. We found that $PKM2^{WT}$ bound more importin α5 than $PKM2^{T405A/S406A}$ did, and the up-regulation of *O*-GlcNAcylation by PUGNAc treatment further improved importin α5 association with $PKM2^{WT}$ (Fig. 4*C*). Interestingly, structural analysis revealed that at the tetramer stage, key residues Arg^{399} and Arg^{400} of the NLS sequence were buried at the C-C tetramerization interface (Fig. S8 *A* and *B*) and could not be accessed by importin α5. However, as *O*-GlcNAcylation induces detetramerization of PKM2, the NLS region is probably exposed to recruit importin α5 which facilitates the nuclear translocation of PKM2.

ERK2-dependent phosphorylation of PKM2 at Ser^{37} has been demonstrated to be required for its nuclear translocation (15). Hence, we wondered if there might be a cross-talk between *O*-GlcNAcylation and phosphorylation on PKM2. As previously reported, the PKM2 mutant whose Ser^{37} was replaced by alanine ($PKM2^{S37A}$) failed to efficiently transport into the nucleus (Fig. 4 *A* and *B*). Interestingly, the mutation at Ser^{37} also abolished the PKM2 nuclear translocation induced by *O*-GlcNAcylation upon PUGNAc treatment (Fig. 4 *A* and *B*). This implied that the nuclear translocation of PKM2 induced by *O*-GlcNAcylation relies on the phosphorylation of Ser^{37}. Furthermore, we found that when *O*-GlcNAcylation was increased in $PKM2^{WT}$ by PUGNAc treatment, PKM2-bound ERK2 responsible for Ser^{37} phosphorylation was increased, with concomitant increase in $PKM2^{WT}$ phosphorylation at Ser^{37} (Fig. 4*D* and Fig. S3*F*). In parallel, the impairment of *O*-GlcNAcylation in $PKM2^{T405A/S406A}$ caused decreased binding of ERK2 to PKM2 and a clear reduction of Ser^{37} phosphorylation regardless of PUGNAc (Fig. 4*D*). In contrast, *O*-GlcNAcylation of PKM2 was largely unaffected when PKM2 Ser^{37} was mutated to alanine or aspartate (Fig. 4*E*). Furthermore, we observed increased levels of PKM2 *O*-GlcNAcylation

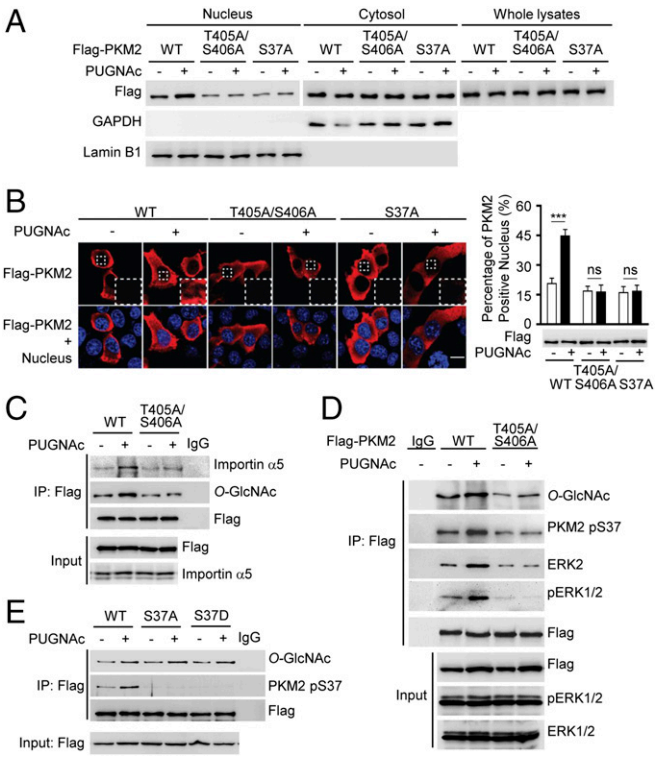

Fig. 4. *O*-GlcNAcylation promotes PKM2 nuclear translocation. Flag-tagged $PKM2^{WT}$, $PKM2^{T405A/S406A}$, $PKM2^{S37A}$, or $PKM2^{S37D}$ was transfected in PKM2 depleted MCF-7 cells along with or without concomitant PUGNAc treatment. (*A*) Fractionation analysis of PKM2. Nuclear, cytoplasmic fractions, and whole lysates were analyzed by WB. Lamin B1 and GAPDH are controls in nuclear and cytosolic fractions. (*B*, *Left*) Cellular localization of PKM2 wild type and mutants by immunofluorescence. (*B*, *Left*, *Insets*) Magnified nucleus. (Scale bar, 10 μm.) (*B*, *Right*) Percentage of cells positive for PKM2 in the nucleus. Error bars, SEM; $n = 30$ (10 fields from each of the three independent experiments). Student's *t* test: $^{***}P < 0.001$; ns, nonsignificant. (*C*) The association of PKM2 with importin α5. Proteins immunoprecipitated by Flag-PKM2 were analyzed by WB. (*D* and *E*) Interplay between *O*-GlcNAcylation and phosphorylation on PKM2. Flag-PKM2–associated proteins were immunoprecipitated and analyzed by WB with the indicated antibodies.

upon EGF treatment, which is known to boost Ser^{37} phosphorylation through activating ERK signaling (Fig. S8*C*). However, in $PKM2^{T405A/S406A}$, EGF-induced Ser^{37} phosphorylation was completely abolished (Fig. S8*C*). Collectively, these data show that *O*-GlcNAcylation at Thr^{405} and Ser^{406} is an event upstream of Ser^{37} phosphorylation.

PKM2 *O*-GlcNAcylation Promotes the Warburg Effect and Cell Proliferation. Having established that *O*-GlcNAcylation impairs the PKM2 activity in the cytoplasm and triggers its nuclear translocation, we next wanted to know whether these *O*-GlcNAcylation–induced changes would promote the Warburg effect. Firstly, reduced PKM2 activity might cause the accumulation of upstream glycolytic metabolites that can be used for lipid and nucleic acid synthesis (2, 4, 32). Indeed, we found that the rate of lipid and DNA synthesis was greatly up-regulated in cells expressing $PKM2^{WT}$ compared with that in cells carrying $PKM2^{T405A/S406A}$ (Fig. S9*A*). Thus, *O*-GlcNAcylation–induced reduction of PKM2 activity may contribute to the Warburg effect by redirecting glycolytic flux toward anabolic pathways.

Secondly, PKM2 migration into nucleus has been shown to induce a HIF-1α– and c-Myc–mediated expression of a series of glycolysis-related regulators, including glucose transporter 1 (Glut1) and lactate dehydrogenase A (LDHA), which are directly responsible for the regulation of glucose consumption and lactate production (15). Indeed, we found that PKM2 *O*-GlcNAcylation signaling was associated with the expression of Glut1 and LDHA: (*i*) upon PUGNAc treatment, $PKM2^{WT}$ enhanced both mRNA and protein levels of Glut1 and LDHA, whereas $PKM2^{T405A/S406A}$ failed to do so (Fig. 5 *A* and *B*); and (*ii*) mutations of residues Arg^{399} and Arg^{400} of the NLS sequence abolished PUGNAc-induced expression of Glut1 and LDHA (Fig. S9 *B* and *C*). As expected, glucose consumption and lactate production were significantly increased by $PKM2^{WT}$, but not $PKM2^{T405A/S406A}$, in the presence of PUGNAc (Fig. S9*D*). This induction could be mediated by c-Myc, as both mRNA and protein levels of c-Myc were increased with $PKM2^{WT}$, but not $PKM2^{T405A/S406A}$ (Fig. S9 *E* and *F*), and an interaction of $PKM2^{WT}$ with the c-Myc promoter region was also observed (Fig. S9*G*). These observations demonstrated that *O*-GlcNAcylation of PKM2 at Thr^{405} and Ser^{406} promoted the Warburg effect by up-regulating the expression of Glut1 and LDHA through a nuclear role via c-Myc. Together, we conclude that *O*-GlcNAcylation of Thr^{405} and Ser^{406} regulates both metabolic and nonmetabolic function of PKM2 to promote the Warburg effect.

We further investigated the impact of PKM2 *O*-GlcNAcylation on cell proliferation by constructing stable MCF-7 cancer cell lines depleted for PKM2 and rescued by either $PKM2^{WT}$ or $PKM2^{T405A/S406A}$. Of note, the expression levels of exogenous PKM2 in these rescue cell lines were comparable (Fig. 5*C*). Compared with cells expressing $PKM2^{WT}$, $PKM2^{T405A/S406A}$ rescue cells displayed a lower growth rate (Fig. 5*D*). We next injected nude mice with these rescue cell lines and assayed for tumor formation. Compared with mice injected with $PKM2^{WT}$, mice injected with $PKM2^{T405A/S406A}$ exhibited decreased tumor volume and mass (Fig. 5 *E*–*G*). In line with the impaired tumor growth in mice injected with $PKM2^{T405A/S406A}$, Ki-67, the classic marker of cell proliferation, was significantly decreased in those tumor tissues (Fig. 5*H*). These data support that *O*-GlcNAcylation of PKM2 at Thr^{405} and Ser^{406} confers a growth advantage for tumor cells in vivo.

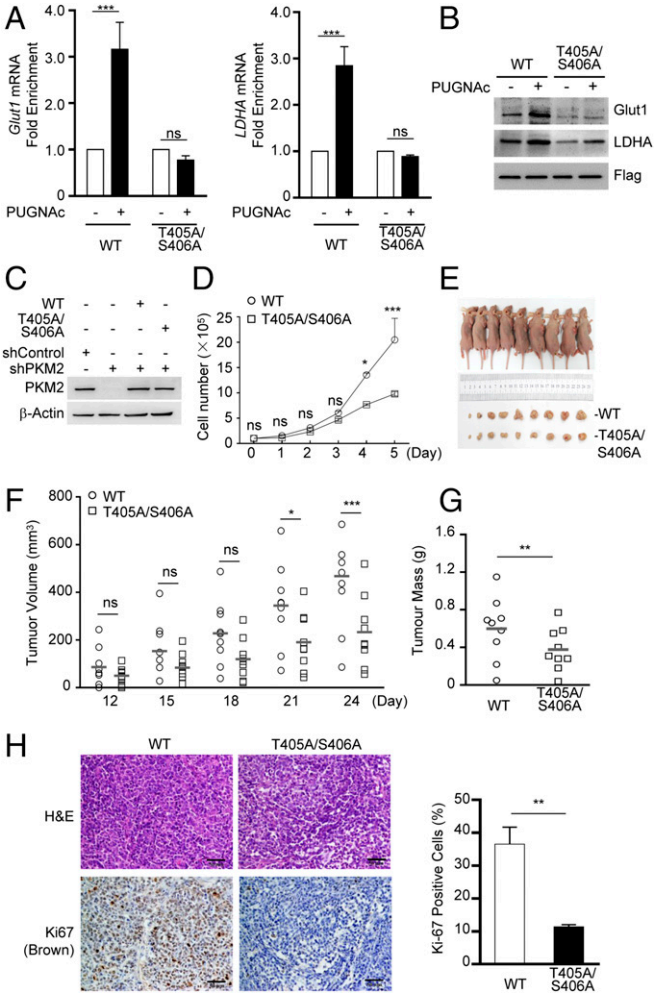

Fig. 5. PKM2 *O*-GlcNAcylation is crucial for the Warburg effect and tumor growth. (*A*) *O*-GlcNAcylation of $PKM2^{WT}$ enhances the mRNA level of Glut1 (*Left*) and LDHA (*Right*). Error bars, SEM; $n = 4$ biological replicas. Student's *t* test: $***P < 0.001$; ns, nonsignificant. (*B*) Protein levels of Glut1 and LDHA were induced by PKM2 *O*-GlcNAcylation. (*C*) Establishment of PKM2 rescue cell lines. MCF-7 cells depleted for endogenous PKM2 were stably reexpressed with exogenous $PKM2^{WT}$ or $PKM2^{T405A/S406A}$. (*D*) Proliferation curves of $PKM2^{WT}$ and $PKM2^{T405A/S406A}$ rescue cell lines. $PKM2^{WT}$ and $PKM2^{T405A/S406A}$ rescue cells were seeded at the same number in each well. Cell numbers were counted every 24 h. Error bars, SEM. Student's *t* test: $*P < 0.05$; $***P < 0.001$; ns, nonsignificant. (*E*–*G*) Tumor formation in nude mice. $PKM2^{WT}$ and $PKM2^{T405A/S406A}$ rescue cells were, respectively, injected into athymic nude mice. The xenograft tumors were sampled and photographed after 24 d. Images of mice bearing tumor are as in *E*. Tumor volumes were measured at the indicated time points as in *F*. According to length (*l*), width (*w*), and height (*h*), volumes were calculated based on the equation $v = lwh\pi/6$. The quantification of the average mass of xenograft tumors was as in *G*. Mean is shown, $n = 9$. Student's *t* test: $*P < 0.05$; $**P < 0.01$; $***P < 0.001$; ns, nonsignificant. (*H*) Immunohistology analysis for cell proliferation. Nine pairs of mice injected with $PKM2^{WT}$ or $PKM2^{T405A/S406A}$ rescue cells were costained with hematoxylin and eosin (H&E) and Ki-67. (*H*, *Left*) Representative images depicting tumor tissues. (Scale bars, 50 μm.) (*H*, *Right*) Quantification of Ki-67 staining. Error bars, SEM; $n = 15$ (five fields from each of the three analyzed mice). Student's *t* test: $**P < 0.01$.

Discussion

Here, we have uncovered a previously unknown mechanism for regulation of PKM2 function by *O*-GlcNAcylation, which simultaneously impinges on both metabolic and nuclear (nonmetabolic) functions of PKM2 to promote the Warburg effect. On the one hand, *O*-GlcNAcylation–dependent detetramerization of PKM2 causes reduced PK activity, which directly rewires metabolic fluxes toward anabolic pathways for rapid cell proliferation. On the other hand, *O*-GlcNAcylation at Thr^{405} and Ser^{406} directly destabilizes PKM2 tetramers to facilitate the exposure of NLS and downstream Ser^{37} phosphorylation for PKM2 nuclear localization. This in turn stimulates c-Myc–dependent expression of two key glycolysis components, namely, Glut1 and LDHA, to enhance glucose consumption and lactate production.

Notably, the *O*-GlcNAcylation residues of PKM2, Thr^{405} and Ser^{406}, are encoded by the alternatively spliced exon 10 and

located at the so-called C-C dimer interface of the PKM2 tetramer (29). Thus, *O*-GlcNAcylation appears to be a unique regulatory mode for PKM2 function which serves as a bridge translating genomic gene expression switch from PKM1 to PKM2 toward metabolic reprogramming. By providing an *O*-GlcNAcylation platform that can adjust the PK structure, the selective expression of PKM2 in rapidly proliferating cells might thus confer certain advantages in the dynamic control of the Warburg effect.

Two metabolic enzymes, PFK1 and G6PD, are known to be regulated by *O*-GlcNAc modification (23, 24). *O*-GlcNAcylation of PFK1 and G6PD redirects metabolic flux through the pentose phosphate pathway (PPP) and rebalances the metabolic need for ribose 5-phosphate and NADPH (23, 24). Depending on the demands for NADPH, ribose 5-phosphate, and ATP, cells are able to select the proper PPP metabolic mode to fine-tune glucose-6-phosphate flux (33). Given that PK catalyzes the last irreversible reaction in glycolysis, PKM2 glycosylation probably facilitates global metabolic readjustment by redirecting metabolites to branching anabolic pathways to meet the extensive needs of proliferating cells. In addition, compared with phosphorylation, acetylation, and SUMOylation, *O*-GlcNAcylation has been recognized as a unique PTM sensing fluctuation in nutrient environment (28, 34–37). By controlling PKM2 structure and function, *O*-GlcNAcylation couples metabolic state to a dynamically changing environment. This previously uncharacterized mechanism represents an efficient means for cells to coordinate metabolic regulation with nutritional dynamics.

Thus, our findings furnish a key element for unraveling the Warburg effect in cancer biology. Alteration of the PKM2 oligomeric state by *O*-GlcNAcylation allows simultaneous control of the metabolic and nuclear (nonmetabolic) roles of this key enzyme in proliferating cells. Importantly, we demonstrate the ubiquity of this regulatory mode across a wide range of cancer cell types and provide direct evidence for an in vivo role in tumor proliferation. These observations make the *O*-GlcNAcylation apparatus a target of great interest, both for understanding tumor metabolism and for potential intervention to limit tumor growth.

Materials and Methods

Reagents, cell lines, patient tissues, cell fractionations and immunoprecipitation, PKM2 *O*-GlcNAcylation assay, PKM2 structure modeling, PKM2 activity assay, lipid and DNA synthesis assay, and immunohistochemistry analysis are described in detail in *SI Materials and Methods*. Human blood samples were obtained from the Jilin Blood Center according to the Standard for Health Examination of Blood Donors (GB18467-2011). Breast tumor tissues and matching tumor-adjacent normal tissues from patients were obtained from the Tissue Bank of China–Japan Union Hospital of Jilin University during surgery and stored at −80 °C. The present study was approved by the Ethical Committee of Jilin Blood Center and China–Japan Union Hospital of Jilin University and conducted with the informed consent of all donors and patients. All animal work procedures were approved by the Animal Care Committee of the Northeast Normal University (Changchun, China).

ACKNOWLEDGMENTS. We thank Drs. Weiwei Yang and Gerald W. Hart for providing useful reagents; Drs. Xianling Cong & Miao Hao (China-Japan Union Hospital of Jilin University) and Dr. Lin Chen (Jilin Blood Center) for human tissues and blood samples; and Drs. Qunying Lei, Baiqu Huang, Bao Liu, Xianlu Zeng, Jun Lu, Shucai Wang, and Yuzhu Dong for critical comments. This work was supported by National Natural Science Foundation of China Grants 31170769 and 31270916; Program for Introducing Talents to Universities Grant B07017; and the Fundamental Research Funds for the Central Universities. L.A. is supported by the intramural research program of the National Library of Medicine, National Institutes of Health.

1. Sullivan LB, Gui DY, Heiden MGV (2016) Altered metabolite levels in cancer: Implications for tumour biology and cancer therapy. *Nat Rev Cancer* 16:680–693.
2. Cairns RA, Harris IS, Mak TW (2011) Regulation of cancer cell metabolism. *Nat Rev Cancer* 11:85–95.
3. Koppenol WH, Bounds PL, Dang CV (2011) Otto Warburg's contributions to current concepts of cancer metabolism. *Nat Rev Cancer* 11:325–337.
4. Vander Heiden MG, Cantley LC, Thompson CB (2009) Understanding the Warburg effect: The metabolic requirements of cell proliferation. *Science* 324:1029–1033.
5. Pavlova NN, Thompson CB (2016) The emerging hallmarks of cancer metabolism. *Cell Metab* 23:27–47.
6. Lunt SY, Vander Heiden MG (2011) Aerobic glycolysis: Meeting the metabolic requirements of cell proliferation. *Annu Rev Cell Dev Biol* 27:441–464.
7. Christofk HR, et al. (2008) The M2 splice isoform of pyruvate kinase is important for cancer metabolism and tumour growth. *Nature* 452:230–233.
8. Dayton TL, Jacks T, Vander Heiden MG (2016) PKM2, cancer metabolism, and the road ahead. *EMBO Rep* 17:1721–1730.
9. Luo W, et al. (2011) Pyruvate kinase M2 is a PHD3-stimulated coactivator for hypoxia-inducible factor 1. *Cell* 145:732–744.
10. Noguchi T, Yamada K, Inoue H, Matsuda T, Tanaka T (1987) The L- and R-type isozymes of rat pyruvate kinase are produced from a single gene by use of different promoters. *J Biol Chem* 262:14366–14371.
11. Noguchi T, Inoue H, Tanaka T (1986) The M1- and M2-type isozymes of rat pyruvate kinase are produced from the same gene by alternative RNA splicing. *J Biol Chem* 261:13807–13812.
12. Jurica MS, et al. (1998) The allosteric regulation of pyruvate kinase by fructose-1,6-bisphosphate. *Structure* 6:195–210.
13. Chaneton B, et al. (2012) Serine is a natural ligand and allosteric activator of pyruvate kinase M2. *Nature* 491:458–462.
14. Lv L, et al. (2011) Acetylation targets the M2 isoform of pyruvate kinase for degradation through chaperone-mediated autophagy and promotes tumor growth. *Mol Cell* 42:719–730.
15. Yang W, et al. (2012) ERK1/2-dependent phosphorylation and nuclear translocation of PKM2 promotes the Warburg effect. *Nat Cell Biol* 14:1295–1304.
16. Lv L, et al. (2013) Mitogenic and oncogenic stimulation of K433 acetylation promotes PKM2 protein kinase activity and nuclear localization. *Mol Cell* 52:340–352.
17. Hitosugi T, et al. (2009) Tyrosine phosphorylation inhibits PKM2 to promote the Warburg effect and tumor growth. *Sci Signal* 2:ra73.
18. Spoden GA, et al. (2009) The SUMO-E3 ligase PIAS3 targets pyruvate kinase M2. *J Cell Biochem* 107:293–302.
19. Anastasiou D, et al. (2011) Inhibition of pyruvate kinase M2 by reactive oxygen species contributes to cellular antioxidant responses. *Science* 334:1278–1283.
20. Yang W, et al. (2011) Nuclear PKM2 regulates β-catenin transactivation upon EGFR activation. *Nature* 480:118–122.
21. Gui DY, Lewis CA, Vander Heiden MG (2013) Allosteric regulation of PKM2 allows cellular adaptation to different physiological states. *Sci Signal* 6:pe7.
22. Clark PM, et al. (2008) Direct in-gel fluorescence detection and cellular imaging of *O*-GlcNAc-modified proteins. *J Am Chem Soc* 130:11576–11577.
23. Rao X, et al. (2015) *O*-GlcNAcylation of G6PD promotes the pentose phosphate pathway and tumor growth. *Nat Commun* 6:8468.
24. Yi W, et al. (2012) Phosphofructokinase 1 glycosylation regulates cell growth and metabolism. *Science* 337:975–980.
25. Khidekel N, et al. (2003) A chemoenzymatic approach toward the rapid and sensitive detection of *O*-GlcNAc posttranslational modifications. *J Am Chem Soc* 125:16162–16163.
26. Rexach JE, et al. (2010) Quantification of *O*-glycosylation stoichiometry and dynamics using resolvable mass tags. *Nat Chem Biol* 6:645–651.
27. Dombrauckas JD, Santarsiero BD, Mesecar AD (2005) Structural basis for tumor pyruvate kinase M2 allosteric regulation and catalysis. *Biochemistry* 44:9417–9429.
28. Ferrer CM, et al. (2014) *O*-GlcNAcylation regulates cancer metabolism and survival stress signaling via regulation of the HIF-1 pathway. *Mol Cell* 54:820–831.
29. Morgan HP, et al. (2013) M2 pyruvate kinase provides a mechanism for nutrient sensing and regulation of cell proliferation. *Proc Natl Acad Sci USA* 110:5881–5886.
30. Hamabe A, et al. (2014) Role of pyruvate kinase M2 in transcriptional regulation leading to epithelial-mesenchymal transition. *Proc Natl Acad Sci USA* 111:15526–15531.
31. Wang HJ, et al. (2014) JMJD5 regulates PKM2 nuclear translocation and reprograms HIF-1α-mediated glucose metabolism. *Proc Natl Acad Sci USA* 111:279–284.
32. Christofk HR, Vander Heiden MG, Wu N, Asara JM, Cantley LC (2008) Pyruvate kinase M2 is a phosphotyrosine-binding protein. *Nature* 452:181–186.
33. Stincone A, et al. (2015) The return of metabolism: Biochemistry and physiology of the pentose phosphate pathway. *Biol Rev Camb Philos Soc* 90:927–963.
34. Hart GW, Slawson C, Ramirez-Correa G, Lagerlof O (2011) Cross talk between *O*-GlcNAcylation and phosphorylation: Roles in signaling, transcription, and chronic disease. *Annu Rev Biochem* 80:825–858.
35. Hart GW, Housley MP, Slawson C (2007) Cycling of *O*-linked beta-*N*-acetylglucosamine on nucleocytoplasmic proteins. *Nature* 446:1017–1022.
36. Wells L, Vosseller K, Hart GW (2001) Glycosylation of nucleocytoplasmic proteins: Signal transduction and *O*-GlcNAc. *Science* 291:2376–2378.
37. Caldwell SA, et al. (2010) Nutrient sensor *O*-GlcNAc transferase regulates breast cancer tumorigenesis through targeting of the oncogenic transcription factor FoxM1. *Oncogene* 29:2831–2842.